

Report LR-779

A Method to account for Partial Leading-Edge Suction and Vortex Flow for Swept and Delta Wings at Subsonic and Supersonic Speeds

December 1994

A.H.W. Bos

A Method to account for Partial Leading-Edge Suction and Vortex Flow for Swept and Delta Wings at Subsonic and Supersonic Speeds

A.H.W. Bos

Copyright © 1994, by Delft University of Technology, Faculty of Aerospace Engineering, Delft, The Netherlands.

All rights reserved. No part of this publication may be reproduced, stored in a retrieval system or transmitted in any form or by any means, electronic, mechanical, photocopying, recording or otherwise, without the prior written permission of the Delft University of Technology, Faculty of Aerospace Engineering, Delft, The Netherlands.

Publisher: Delft University of Technology
Faculty of Aerospace Engineering
P.O. Box 5058
2600 GB Delft
The Netherlands.
tel: (015)782058
fax: (015)781822

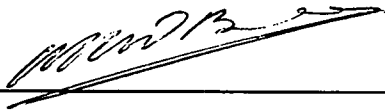
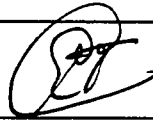

ISBN: 90-5623-004-2

Organization : TUD/LR/A2L

Date: December 1994

Document code : LR-779

Title	:	A method to account for partial leading-edge suction and vortex flow for swept and delta wings at subsonic and supersonic speeds
Author(s)	:	A.H.W. Bos
Abstract	:	Based on the Polhamus leading-edge suction analogy and the Carlson attainable thrust concept, closed-form relations are derived which provide a means to calculate the lift and drag coefficient of flat swept or delta wings. The partial loss of the leading-edge suction force caused by flow separation and the resulting occurrence of leading-edge vortices have been taken into account. The method is valid both in subsonic and supersonic flow.
Keyword(s)	:	leading-edge suction, attainable thrust concept, leading-edge vortices

Date	December 1994	
Prepared	A.H.W. Bos	
Verified		
Approved	E. Torenbeek	
Authorized EB	P.G. Bakker	

Summary

In this report, based on the Polhamus leading-edge suction analogy and the Carlson attainable thrust concept, closed-form relations are derived which provide a means to calculate the lift and drag coefficient of flat swept or delta wings. The partial loss of the leading-edge suction force caused by flow separation and the resulting occurrence of leading-edge vortices have been taken into account. The method is valid both in subsonic and supersonic flow.

Contents

	page
Summary	i
Notation	iii
1. Introduction	1
2. Leading-edge suction analogy	3
3. Attainable thrust concept	12
4. Application to double-delta wings	22
5. Results	25
6. Conclusions	34
References	35
Appendix	37

Notation

A	aspect ratio (b^2/S)
b	wing span
C_D	drag coefficient (3D)
C_L	lift coefficient (3D)
C_{L_α}	lift gradient (3D)
C_N	normal force coefficient (3D)
C_S	suction force coefficient normal to leading-edge (3D)
C_T	thrust (suction force) coefficient (3D)
C_X	tangential force coefficient (3D)
c	chord
c_d	drag coefficient (2D)
c_l	lift coefficient (2D)
c_{l_α}	lift gradient (2D)
c_n	normal force coefficient (2D)
c_p	pressure coefficient
$(\Delta c_p \sqrt{x})_0$	limiting value of leading-edge pressure coefficient
c_s	suction force coefficient perpendicular to leading-edge (2D)
c_t	local thrust (suction force) coefficient
D	drag
E	elliptical integral of the second kind
i_w	wing angle of incidence
K_A	attainable thrust factor
\bar{K}_A	average attainable thrust factor over span
K_T	leading-edge thrust factor
K_V	vortex flow factor
K_i	induced downwash factor
K_p	lift gradient in potential flow
$k_1 - k_4$	profile definition coefficients
L	lift
l	lift per unit span
l_i	spanwise location of wing kink measured from root
M	Mach number
M_e	equivalent Mach number for vacuum limiting pressure
m	leading-edge parameter
N	normal force
n	normal force per unit span
R_e	Reynolds number based on chord
R_n	Reynolds number based on normal chord
r	leading-edge nose radius
S	wing area
s	semi net wing span
T	thrust force
t	local thrust force
	tangential force per unit span
	wing thickness
U	free stream velocity

w_i	induced downwash velocity
x	chordwise profile coordinate
y	spanwise coordinate
	profile thickness coordinate
α	angle of attack
Γ	circulation strength
γ	specific heat ratio of air
η	power in approximation of elliptical integral
Δ	sweep angle
μ	Mach angle
ρ	density of air
ϕ	angle in definition of elliptical integral
	wing span efficiency factor

subscripts

0	at profile leading-edge
i	inner
	induced
le	leading-edge
n	normal to wing leading-edge in wing plane
o	outer
p	potential
v	vortex
w	wing

1. Introduction

Since the design of airplanes capable of cruising at supersonic speeds involves finding a compromise between the contradicting performance requirements at high-speed flight and low-speed flight, it is very important to be able to predict the aircraft's characteristics accurately throughout the operational envelope. Therefore, especially for wave drag calculations of configurations somewhat more complicated than the pure delta wing, more advanced aerodynamic models than handbook methods like the USAF Stability and Control DATCOM are often used. Also, in the case of wings with a supersonic leading-edge, in those regions where Evvard's principle applies (the area between the Mach line from the tip leading-edge, the tip chord and the trailing-edge), the pressure distribution differs from the two-dimensional case (constant loading) which applies elsewhere on the section with the supersonic leading-edge. In order to account for this effect in the lift and drag calculations, a method based on the near-field integration of the perturbation potential, for instance a panel method, is needed. Furthermore, as far as the subsonic case is concerned, many handbook methods have a limited applicability, usually with respect to moderate sweep angles and not too small aspect ratios.

Unfortunately, even the more advanced computational aerodynamic models do not fully account for an effect that is very important in the analysis of wings that are especially designed for high speeds. In subsonic flow a leading-edge suction force occurs on leading-edges that are sufficiently rounded off. Depending on the leading-edge sweep angle of the wing, this force can be retained in supersonic flow, provided that the leading-edge flow remains subsonic. As, in supersonic cruise, lift-to-drag ratio's tend to be relatively low because of the presence of wave drag, this can be very worthwhile for vehicles designed for long range.

If the leading-edge radius of the wing is small, however, the suction force cannot be generated as the flow around the nose will separate, resulting in large vortices over the wing. This will especially occur at high angles of attack, for instance during the landing approach, where the vortex flow will provide a large amount of extra lift, thus enabling a lower approach speed and accordingly shorter landing field length. As the aspect ratio of the wing for supersonic cruising airplanes is usually relatively small, leading to high approach angle of attacks, this is an important effect. The disadvantage of the development of vortex flow is, however, that it results in a large increase in drag, as on the one hand the suction force disappears, while on the other hand an extra component of induced drag is generated.

At present, the only methods that are capable of taking these effects into account are specially adapted panel methods or Euler methods. Since these methods require far too much computational time to be suitable in the conceptual stage of the design proces, other means have to be employed to take this phenomenon into account, which is very important for supersonic airplanes. The purpose of the present report is to summarize

available methods from literature, especially from [ref.3], [ref.4], [ref.12] and [ref.13] and to use these in combination with a panel method (linearized potential flow) used at the Delft University of Technology, the NLRAERO program, developed by the National Aerospace Laboratory NLR ([ref.8], [ref.9] and [ref.11]).

2. Leading-edge suction analogy

A very useful, though not entirely physically supported, theory to predict drag and lift due to leading-edge vortices is the so-called leading-edge suction analogy, introduced by Polhamus ([ref.12] and [ref.13]). The basis for this theory is the assumption, that the force required to maintain the reattached flow behind the vortex is equal to the force required to maintain the attached potential flow around the leading-edge. If this is the case, then the lift and drag due to the vortex flow can be found by calculating the leading-edge suction force as it occurs in potential flow and rotating it 90 degrees upward. It has been established that this theory accounts very well for the strong non-linear behaviour of the lift coefficient as observed in windtunnel tests with highly swept, sharp leading-edge wings.

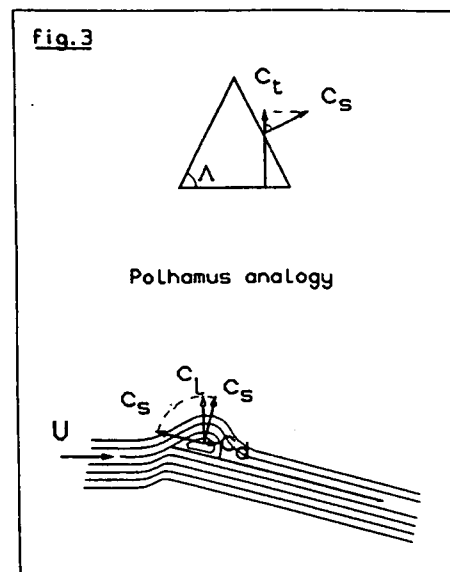
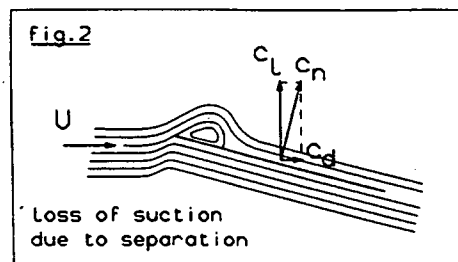
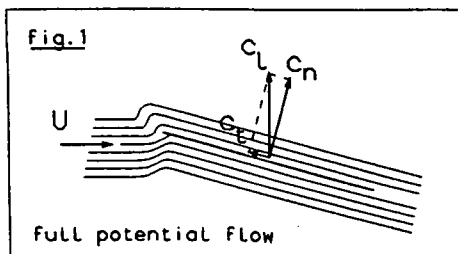


fig.1,2 and 3 Polhamus leading-edge suction analogy

Subsonic flow

In two-dimensional potential flow, using Blasius' theorem, the following two expressions can be derived for the tangential and the normal force per unit span, acting on a flat plate:

$$t = \rho U \Gamma \sin \alpha \quad (1)$$

$$n = \rho U \Gamma \cos \alpha \quad (2)$$

The circulation Γ follows from the Kutta-condition, which ensures a smooth, attached trailing-edge flow:

$$\Gamma = \pi U c \sin \alpha \quad (3)$$

Thus, the lift per unit span equals:

$$l = \rho U \Gamma \quad (4)$$

or:

$$c_l = 2\pi \sin \alpha \quad (5)$$

In two-dimensional potential flow, the drag force equals zero (d'Alembert's paradox, fig.1).

If, due to separation at a sharp leading-edge the suction force disappears, the following results are obtained (fig.2):

$$c_n = \frac{\rho U \Gamma \cos \alpha}{\frac{1}{2} \rho U^2 c} = 2\pi \sin \alpha \cos \alpha \quad (6)$$

$$c_l = c_n \cos \alpha = 2\pi \sin \alpha \cos^2 \alpha \quad (7)$$

$$c_d = c_n \sin \alpha = 2\pi \sin^2 \alpha \cos \alpha \quad (8)$$

Hereafter, these expressions will be given the subscript p, as they represent the potential-flow contribution.

According to the Polhamus leading-edge suction analogy, the contribution to drag and lift due to the vortex flow, can be derived by taking the theoretical potential-flow suction force that acts perpendicular to the leading-edge and rotate it 90 degrees upward (fig.3):

$$c_{l_v} = c_s \cos \alpha = \frac{c_t}{\cos \Lambda} \cos \alpha = \frac{2\pi}{\cos \Lambda} \sin^2 \alpha \cos \alpha \quad (9)$$

$$c_{d_v} = c_{l_v} \tan \alpha \quad (10)$$

In three-dimensional flow, the drag is not zero. Due to the trailing vortices, an effective downwash velocity is induced, normal to the chord. This will cause a reduction of the magnitude of the suction force, according to:

$$T = \rho \Gamma b (U \sin \alpha - w_i) \quad (11)$$

The circulation strength is still determined by the Kutta-condition:

$$\Gamma = \frac{K_p}{2} U \frac{S}{b} \sin \alpha \quad (12)$$

Comparison with the expressions for two-dimensional potential flow shows that K_p is equal to the lift-gradient C_{L_α} .

Substitution yields for the suction force coefficient:

$$C_T = \left(1 - \frac{w_i}{U \sin \alpha} \right) K_p \sin^2 \alpha \quad (13)$$

As the downwash depends on the circulation strength only, which according to the Kutta-

condition is determined by $U \sin \alpha$, the following relation may be introduced:

$$\frac{w_i}{U \sin \alpha} = K_p K_i \quad (14)$$

Then the following expression is found for the suction force coefficient in three-dimensional potential flow:

$$C_T = (K_p - K_p^2 K_i) \sin^2 \alpha \approx \left(\frac{\partial C_T}{\partial \alpha^2} \right) \alpha^2 \quad (15)$$

The three-dimensional vortex contribution to the lift coefficient can then be expressed as:

$$C_{L_v} = K_v \sin^2 \alpha \cos \alpha \quad (16)$$

with:

$$K_v = \left(\frac{\partial C_T}{\partial \alpha^2} \right) \frac{1}{\cos \Lambda_{1e}} \quad (17)$$

The induced drag in three-dimensional potential flow is equal to:

$$C_{D_i} = C_N \sin \alpha - C_T \cos \alpha \quad (18)$$

The ratio of these two terms is shown in fig.4 which stresses the importance of retaining the leading-edge suction force. It is obvious that in subsonic flow, the suction force can be quite substantial and cause a large reduction of the induced drag. In supersonic flow, on the other hand, although the suction force in comparison to the potential flow contribution to the drag is not as large, very significant reductions of the induced drag can be realized through geometrical adaptations.

With the previously deduced expressions, equation (18) may be written as:

$$C_{D_i} = C_{L_\alpha} \sin^2 \alpha \cos \alpha - C_T \cos \alpha \quad (19)$$

or:

$$C_{D_i} \approx \alpha^2 C_{L_\alpha} - C_T = C_L^2 \left(\frac{1}{C_{L_\alpha}} - \frac{C_T}{C_L^2} \right) \quad (20)$$

using $C_L \approx C_{L_\alpha} \alpha$, which applies in linearized flow. As, in subsonic flow, the induced drag of flat wings can be expressed as $C_{D_i} = \frac{C_L^2}{\pi A \phi}$, the following results can be obtained ([ref.10]):

$$C_T = \alpha^2 \left(C_{L_\alpha} - \frac{C_{L_\alpha}^2}{\pi A \phi} \right) \quad (21)$$

$$\Rightarrow \frac{\partial C_T}{\partial \alpha^2} = C_{L_\alpha} - \frac{C_{L_\alpha}^2}{\pi A \phi} \quad (22)$$

$$\Rightarrow K_v = \left(C_{L_\alpha} - \frac{C_{L_\alpha}^2}{\pi A \phi} \right) \frac{1}{\cos \Lambda_{1e}} \quad (23)$$

If the subsonic lift gradient and the induced drag or the span efficiency factor ϕ have been determined either from a panel method or from a simple approximating expression, the vortex coefficient can be calculated.

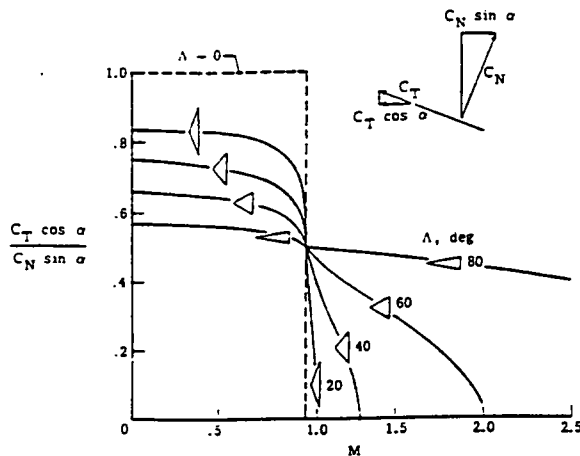


fig.4 normal force and suction force contribution to induced drag ([ref.3])

Supersonic flow

In [ref.6] it is concluded that although leading-edge forces are not large in supersonic flow, they can have a significant influence on the design. Especially the severely twisted and cambered designs resulting from methods that do not take the leading-edge thrust into account could be replaced by more moderate surfaces once it is acknowledged that the leading-edge thrust does not equal zero.

For supersonic flow, an expression for the local suction force coefficient is given in [ref.3] (originally from [ref.2]) for flat delta wings:

$$c_t = \frac{\pi b}{8 S} \tan \Lambda_{le} \sqrt{1 - m^2} (\Delta c_p \sqrt{x})_0^2 \quad (24)$$

based on the mean geometric chord, in which the last term represents the limiting value of the pressure coefficient on the leading-edge. An empirical relation to estimate this value

was given as:

$$(\Delta c_p \sqrt{x})_0 = \frac{4 \sin \alpha}{\sqrt{2}} \frac{\sqrt{y \cot \Lambda_{1e}}}{E} \quad (25)$$

in which E is the elliptical integral of the second kind defined as:

$$E(m) = \int_0^{\pi/2} \sqrt{1 - (1 - m^2) \sin^2 \phi} \, d\phi \quad (26)$$

According to [ref.3], this integral can be approximated as:

$$E = 1 + \left(\frac{\pi}{2} - 1 \right) m^\eta, \quad \eta = 1.226 + 0.15\pi(1 - \sqrt{m}). \quad (27)$$

Substituting equation (25) into equation (24) yields for the local suction force coefficient:

$$c_t = \frac{\pi A \sqrt{1 - m^2}}{E^2} \frac{y}{b} \sin^2 \alpha \quad (28)$$

Integration over the wing span yields the following expression for the supersonic suction force on delta wings:

$$C_T = \frac{\pi A}{4E^2} \sin^2 \alpha \sqrt{1 - m^2} \quad (29)$$

The relation for the limiting value of the pressure coefficient is based on theoretical results. In reality, it was found that these theoretical values often overestimated the suction forces. In order to cope with this problem, Carlson in [ref.4] introduced a method to correlate theoretical values of subsonic and supersonic suction force coefficients with windtunnel experiments. This method has become known as the Carlson attainable thrust concept, which will be explained later.

An expression for the vortex coefficient in supersonic flow can be derived from equations (17) and (29):

$$K_v = \frac{\pi A \sqrt{1-m^2}}{4E^2 \cos \Lambda_{le}} \quad (30)$$

For a delta wing this becomes:

$$K_v = \frac{\pi A \sqrt{1-m^2}}{4E^2} \sqrt{1 + \frac{16}{A^2}} \quad (31)$$

The parameter $m = \frac{\cot \Lambda_{le}}{\tan \mu}$, with μ as Mach angle. For sonic leading-edges, the parameter m becomes 1.

As stated before, the potential flow coefficient K_p is equal to the lift gradient. In supersonic flow, according to [ref.14], this coefficient can be taken as:

$$K_p = \frac{2\pi m}{E \sqrt{M^2-1}} \quad (32)$$

in which E is the previously defined elliptical integral of the second kind.

For a sonic leading-edge (or supersonic, as long as m is kept equal to 1), this relation changes into:

$$K_p = \frac{4}{\sqrt{M^2-1}} \quad (33)$$

which is in accordance with Ackeret's linearized supersonic theory. For a delta wing the relation for K_p becomes:

$$K_p = \frac{\pi A}{2E} \quad (34)$$

In order to obtain the lift and drag-due-to-lift coefficient in a flow with leading-edge vortices, the contributions from the potential flow without leading-edge suction and the Polhamus leading-edge suction analogy are to be added:

$$C_L = C_{L_p} + C_{L_v} = K_p \sin \alpha \cos^2 \alpha + K_v \sin^2 \alpha \cos \alpha \quad (35)$$

$$C_D = C_L \tan \alpha = K_p \sin^2 \alpha \cos \alpha + K_v \sin^3 \alpha \quad (36)$$

3. Attainable Thrust Concept

According to Carlson ([ref.3], [ref.4], [ref.5] and [ref.6]), for a family of symmetric airfoils defined by $y = \pm(k_1\sqrt{x} + k_2x + k_3x^{3/2} + k_4x^2)$ an expression can be derived for a factor K_A which is the ratio between the attainable and the theoretical local suction coefficient:

$$C_{tA} = K_A \cdot C_t \quad (37)$$

In figure 5 a typical pressure distribution is sketched on the left hand side for an airfoil at large angle of attack. The theoretical pressure peak can become quite large, often in excess of the vacuum pressure coefficient, which is obviously unrealistic. In case the pressure coefficient is limited, the picture as sketched at the right hand side of figure 5 remains.

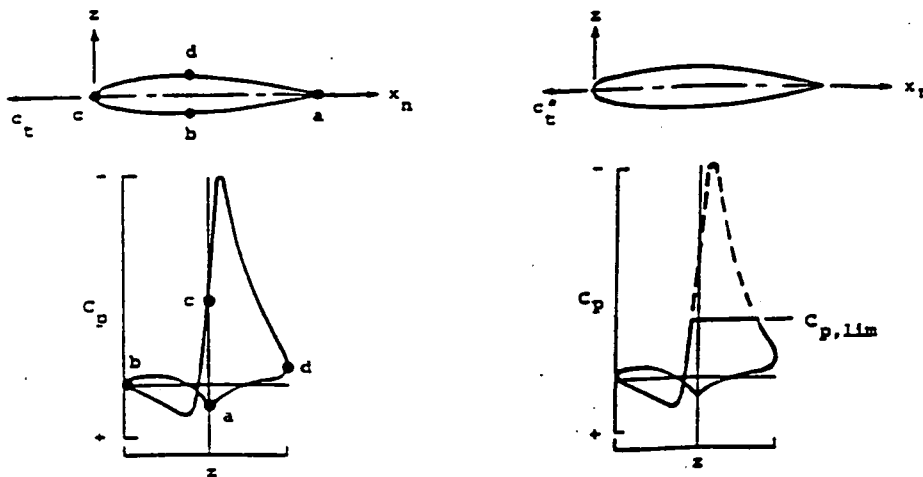


fig.5 typical pressure distribution of airfoil at large angle of attack ([ref.4])

According to [ref.5] limiting the pressure peak to practically achievable pressures has a relatively insignificant effect on the normal force but it severely limits the value of the theoretical suction force, which will therefore be corrected according to equation (37).

Carlson and coworkers found that this attainable thrust coefficient correlated well with the parameter:

$$\frac{c_{t_n} \sqrt{1 - M_n^2}}{\left(\frac{t}{c}\right)_n \left(\frac{r}{c}\right)_n^{0.4}} \quad (38)$$

For the attainable thrust coefficient the following relation was found ([ref.4]):

$$K_A = \frac{2(1 - M_n^2)}{M_n} \left[\frac{\left(\frac{t}{c}\right)_n \left(\frac{r}{c}\right)_n^{0.4}}{c_{t_n} \sqrt{1 - M_n^2}} \right]^{0.6} \quad (39)$$

This relation is depicted in fig.6.

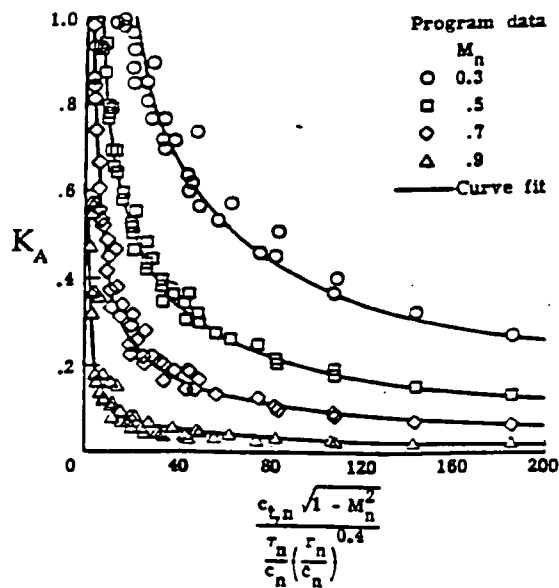


fig.6 attainable thrust factor ([ref.4])

The subscripts n refer to parameters normal to the leading-edge at a selected spanwise station of the original wing. The reasoning behind this is that the flow conditions normal to the wing leading-edge are considered to determine the leading-edge flow behaviour. To obtain these parameters, a phantom wing is superimposed over the original wing in such a way that the leading-edge and trailing-edge sweep angles are equal to those of the original wing (see fig.7, taken from [ref.4]). The maximum thickness line of the phantom wing is chosen such, that it runs through the maximum thickness location of the original wing at the selected spanwise location, while the maximum thickness of the normal section of the phantom wing is placed at midchord. The required airfoil parameters follow by means of simple geometrical relations, which can be found in [ref.4].

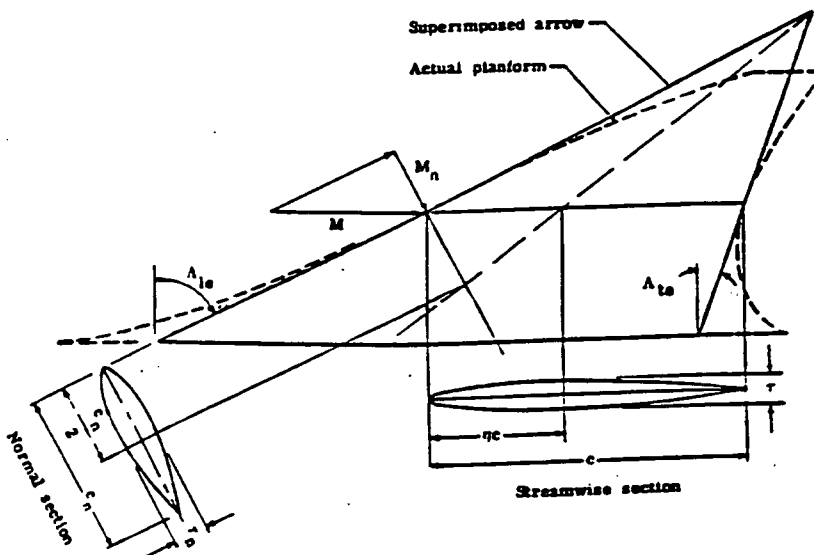


fig.7 definition of normal chord section

Equation (39) was derived for a vacuum limiting pressure. It can be extended to more realistic limiting pressures, as experienced in windtunnel tests, by means of the Prandtl-Glauert rule: the vacuum pressure which occurs at a certain equivalent Mach number M_e , can be related to an arbitrary limiting pressure at the normal Mach number under consideration subject to the following condition:

$$c_{Plim}(M_e) = c_{Plim}(M_n) \frac{\sqrt{1-M_n^2}}{\sqrt{1-M_e^2}} \quad (40)$$

If the limiting pressure coefficient at the equivalent Mach number is set equal to the vacuum pressure coefficient, the following relations hold:

$$K_A = \frac{2(1 - M_e^2)}{M_e} \left[\frac{\left(\frac{t}{c}\right)_n \left(\frac{r}{c}\right)_n^{0.4}}{c_{t_n} \sqrt{1 - M_n^2}} \right]^{0.6} \quad (41)$$

with:

$$M_e = \frac{-\sqrt{2}}{\gamma c_{P_{lim}} \sqrt{1 - M_n^2}} \sqrt{\sqrt{1 + \left(\gamma c_{P_{lim}} \sqrt{1 - M_n^2}\right)^2} - 1} \quad (42)$$

By examining various different profiles at a wide range of Mach numbers and Reynolds numbers in the windtunnel, Carlson derived the following empirical relation for the limiting pressure coefficient:

$$c_{P_{lim}} = \frac{-2}{\gamma M_n^2} \left(\frac{R_n \cdot 10^{-6}}{R_n \cdot 10^{-6} + 10^{4-3M_n}} \right)^{0.05 + 0.35(1 - M_n)^2} \quad (43)$$

The Reynolds numbers in this expression are based on the mean aerodynamic chord and transformed to a chord normal to the leading-edge, again using simple geometrical relations. The correlation of the limiting pressure coefficient with the normal Mach number and Reynolds number is shown in fig.8 which was taken from [ref.4].

In case the factor K_A becomes greater than 1, it is kept equal to 1 (the attainable suction force is never allowed to exceed the theoretical value).

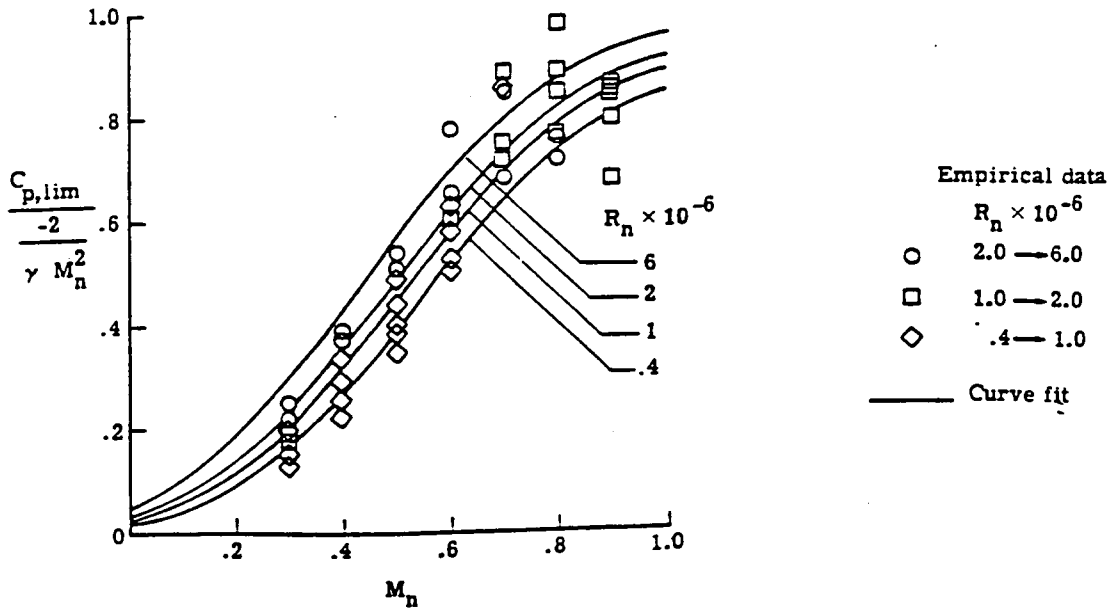


fig.8 limiting pressure coefficient

Instead of calculating the attainable thrust factor for a large number of spanwise locations and integrating over the span, in this application one representative arrow wing is selected, leading to an average value \bar{K}_A . Consequently, for double-delta wings, this could imply that in some cases where the average normal Mach number is supersonic, no suction force is taken into account, although locally some wing sections might be sufficiently swept to generate leading-edge suction. Therefore, in the next section, alternative relations will be presented for double-delta wings.

In case the theoretical suction force is not fully developed ($\bar{K}_A < 1$), for instance because the leading-edge radius is too small, it is assumed that the theoretical suction force vector is rotated upwards in such a way that the tangential force is equal to (see fig.9):

$$\Delta C_X = -\bar{K}_A C_T \tag{44}$$

This causes an extra normal force (compare with Polhamus' leading-edge suction analogy) that is equal to:

$$\Delta C_N = \frac{C_T}{\cos \Lambda_{le}} \sin(\arccos K_A) \quad (45)$$

or:

$$\Delta C_N = \frac{\left(\frac{\partial C_T}{\partial \alpha^2}\right)}{\cos \Lambda_{le}} \sin^2 \alpha \sqrt{1 - K_A^2} \quad (46)$$

For a representative arrow or delta wing this can be written as:

$$\Delta C_L = K_v \sin^2 \alpha \cos \alpha \sqrt{1 - K_A^2} \quad (47)$$

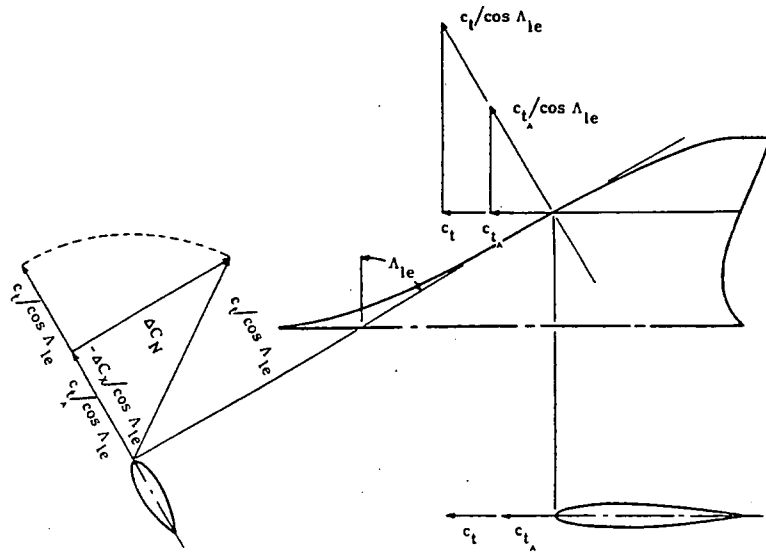


fig.9 attainable thrust concept ([ref.4])

Using in this fashion Polhamus' leading-edge suction analogy and Carlson's attainable leading-edge thrust concept it is possible to combine both effects, suction force and vortex flow, into simple formulas for lift and lift dependent drag of flat wings:

$$C_L = K_p \sin \alpha \cos^2 \alpha + K_T K_A \sin^3 \alpha + K_V \sqrt{1 - K_A^2} \sin^2 \alpha \cos \alpha \quad (48)$$

$$C_D = K_p \sin^2 \alpha \cos \alpha - K_T K_A \sin^2 \alpha \cos \alpha + K_V \sqrt{1 - K_A^2} \sin^3 \alpha \quad (49)$$

In these expressions, the thrust force coefficient was replaced by:

$$C_T = K_T \sin^2 \alpha, \text{ with:}$$

$$K_T = \frac{\pi A}{4E^2} \sqrt{1 - m^2} \text{ for supersonic flow, and}$$

$$K_T = (K_p - K_p^2 K_i), \text{ or } K_T = \left(K_p - \frac{K_p^2}{\pi A \phi} \right) \text{ in subsonic flow.}$$

As, for supersonic flow, both the local suction force coefficient and the attainable thrust coefficient depend on the spanwise coordinate y , an average value should be deduced in order to justify the previous notation. The attainable suction coefficient is defined as:

$$C_{T_A} = \frac{2}{S} \int_0^{b/2} K_A(y) c_t \frac{S}{b} dy \quad (50)$$

Substituting equation (28) then yields:

$$C_{T_A} = \frac{2\pi}{SE^2} \sqrt{1 - m^2} \sin^2 \alpha \int_0^{b/2} y K_A(y) dy = K_T K_A \sin^2 \alpha \quad (51)$$

In order to keep the supersonic suction force coefficient constant at its value at full suction ($K_A = 1$; $K_T = \frac{\pi A}{4E^2} \sqrt{1 - m^2}$), the average attainable thrust coefficient should be based on $y = 0.552 s_w$ (see Appendix).

The relation for the local suction force coefficient (based on the mean chord) as it features in the formula for the attainable suction coefficient is:

$$c_t = \frac{\pi A}{E^2} \sqrt{1-m^2} \left(\frac{\bar{y}}{2s_w} \right) \sin^2 \alpha \quad (52)$$

It should be noted that K_A also depends on the angle of attack. In order to treat it purely as a factor on the total suction force, this dependency was not elaborated in the above expressions, but kept within the definition of K_A . Should this definition of K_A be substituted, however, then it would turn out that the suction force term is proportional to $\sin^{4/5} \alpha$.

For supersonic flow, the two extreme cases will be compared hereafter:

Full leading-edge suction (no vortex lift $K_A = 1$)

$$C_D = K_P \sin^2 \alpha \cos \alpha - K_T \sin^2 \alpha \cos \alpha \quad (53)$$

$$K_T = \frac{\pi A}{4E^2} \sqrt{1-m^2} \quad (54)$$

$$K_P = \frac{\pi A}{2E} \quad (55)$$

Substituting $\alpha = \frac{C_L}{K_P}$ (which is only valid in linearized potential flow, but may be used here as no non-linear vortex flow occurs) the following expression is obtained:

$$C_D = \frac{C_L^2}{\pi A} \left(2E - \sqrt{1-m^2} \right) \quad (56)$$

No leading-edge suction (full vortex lift $K_A=0$)

This situation may occur when sharp airfoils (zero leading-edge radius) are applied.

$$C_D = K_p \sin^2 \alpha \cos \alpha + K_v \sin^3 \alpha \approx K_p \alpha^2 + K_v \alpha^3 \quad (57)$$

Substituting $\alpha = \frac{C_{Lp}}{K_p}$ yields, with equation (30) and $K_p = \frac{\pi A}{2E}$:

$$C_D = \frac{C_{Lp}^2}{\pi A} 2E \left(1 + \frac{\sqrt{1-m^2}}{\pi A \cos \Lambda_{le}} C_{Lp} \right) \quad (58)$$

Since

$$C_L = C_{Lp} \left(1 + \frac{C_{Lv}}{C_{Lp}} \right) = C_{Lp} + C_{Lp}^2 \frac{K_v}{K_p^2} \quad (59)$$

the following expression can be obtained after solving for C_{Lp} :

$$C_{Lp} = \frac{2C_L}{1 + \sqrt{1 + 4 \frac{\sqrt{1-m^2}}{\pi A \cos \Lambda_{le}} C_L}} \quad (60)$$

Substituting this, after some rewriting, the following formula for the total induced drag of a wing developing non-linear lift according to the Polhamus leading-edge suction

analogy is derived:

$$C_D = \frac{C_L^2}{\pi A} \frac{4E}{1 + \sqrt{1 + 4 \frac{\sqrt{1-m^2}}{\pi A \cos \Lambda_{1e}} C_L}} \quad (61)$$

Notice that the lift coefficient now features in the denominator as well. It can be verified easily that if the vortex coefficient becomes zero (e.g. because the leading-edge of the wing

becomes sonic, resulting in m becoming equal to one), the drag equals $C_D = \frac{C_L^2}{K_p}$.

4. Application to double-delta wings

For double-delta wings, the integration of the product of the local supersonic suction force coefficient and the attainable thrust coefficient should be carried out over the panel inboard of the kink and over the panel outboard of the kink (see fig.10). Substituting equation (28) in both parts of the integral yields:

$$C_T = (K_{T_i} + K_{T_o}) \sin^2 \alpha \quad (62)$$

$$K_{T_i} = \frac{\pi A}{4E_i^2} \sqrt{1 - m_i^2} \left(\frac{l_i}{s_w} \right)^2 \quad (63)$$

$$K_{T_o} = \frac{\pi A}{4E_o^2} \sqrt{1 - m_o^2} \left(1 - \left(\frac{l_i}{s_w} \right)^2 \right) \quad (64)$$

For each panel an average value for K_A as well as for K_T must be selected. The value for the average inner attainable thrust coefficient should be based on (see Appendix):

$$\bar{y} = 0.552 l_i \quad (65)$$

whereas the average outer attainable thrust coefficient should be based on:

$$\bar{y} = 0.552 s_w \left(\frac{1 - \left(\frac{l_i}{s_w} \right)^2}{1 - \left(\frac{l_i}{s_w} \right)^{7/5}} \right)^{5/3} \quad (66)$$

in which l_i is the span of one inboard wing panel, measured from the wing root to the spanwise location of the kink (see fig.10).

In case of the presence of a fuselage, it should be noted that K_{T_i} and K_{T_o} are based on the net wing area (integration was performed over the wetted wing span).

In the present context, it is assumed that the thickness-to-chord ratios and the nose radii for the wing profiles are constant for the entire wing. If this is not the case, either average values can be taken, or the spanwise variation can be implemented in the integration.

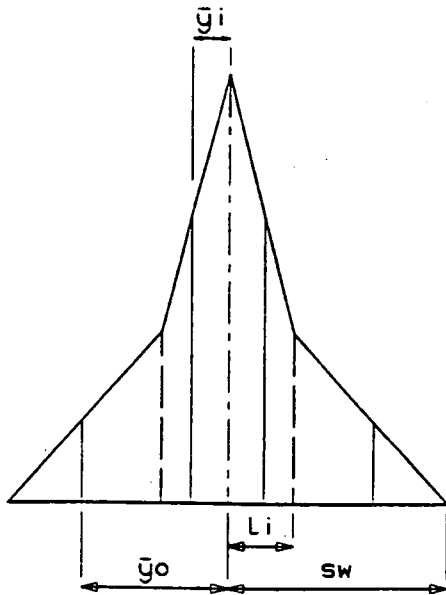


fig.10 double delta wing geometry definition

For subsonic flow, the relations for K_T (based on the gross wing area) become:

$$K_{T_i} = (K_p - K_i K_p^2) \left(\frac{l_i}{s_w} \right) \quad (67)$$

$$K_{T_o} = (K_p - K_i K_p^2) \left(1 - \frac{l_i}{s_w} \right) \quad (68)$$

In case the leading-edge of the outer wing panel is supersonic, the lift gradient should be

split as well. Using the previously introduced expression for K_p this becomes:

$$K_p = \frac{2\pi}{\sqrt{M^2-1}S} \left(\frac{m_i S_i}{E_i} + \frac{m_o S_o}{E_o} \right) \quad (69)$$

If a fuselage is present, the lift gradient is based on the gross wing area. If supersonic tip effects are to be taken into account as well, the lift gradient should be obtained from a panel method, as explained in the introduction.

5. Results

For a pure delta wing values of the attainable thrust coefficient as a function of the nose radius are presented in fig.11. The attainable suction force coefficient, as discussed earlier, is not permitted to exceed the theoretical value. The influence of the nose-radius is obvious.

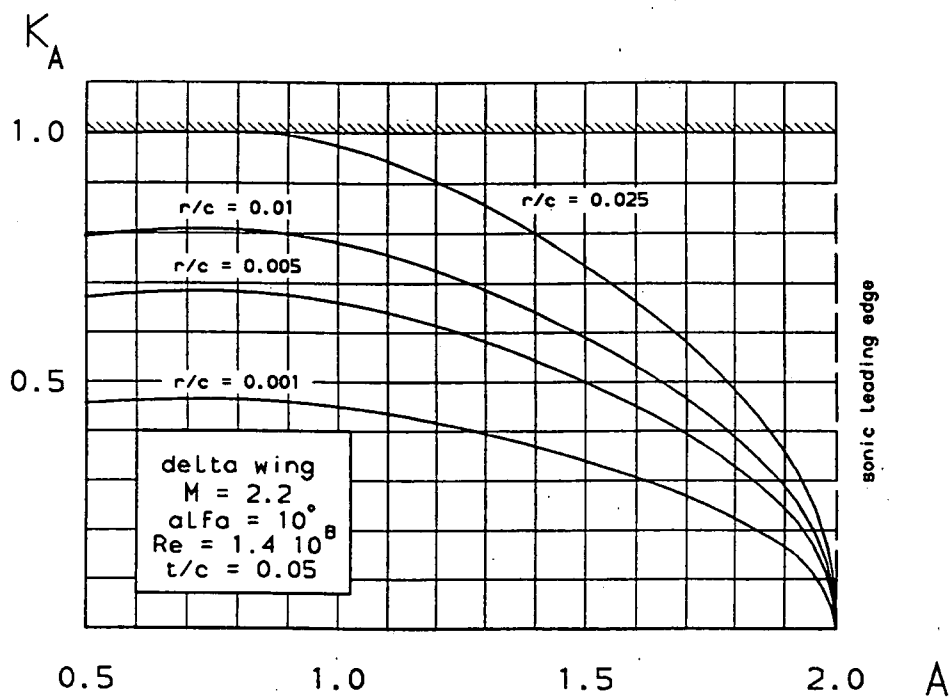


fig.11 attainable thrust coefficient for a family of pure delta wings at $M=2.2$

The ratio of the lift-to-drag ratio's for both extreme values of the attainable thrust coefficient in supersonic flow is shown in fig.12, for a pure delta wing with unit aspect ratio.

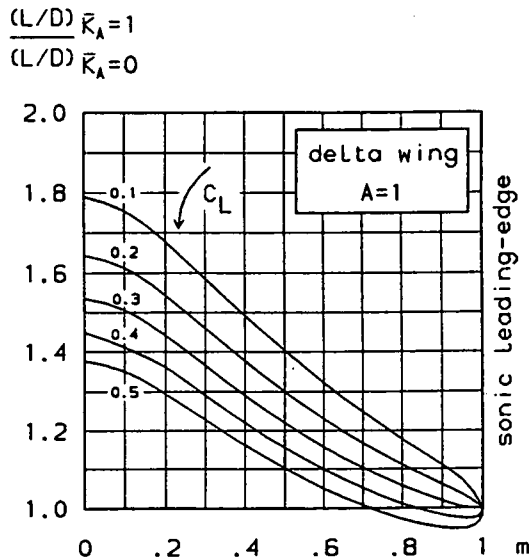


fig.12 ratio of full suction and full vortex L/D for a pure delta of unit aspect ratio

As might be expected, for low values of the lift coefficient, the presence of leading-edge vortices will lead to poor lift-to-drag ratios due to the increased amount of drag. However, at large values of the lift coefficient, a region exists in which the vortex flow seems to be more efficient. Profiles with small leading-edge radii do not seem able to compete with profiles equipped with round leading-edges, as far as maximum lift-to-drag ratio is concerned, as the favourable region is that of high angles of attack, at values which will in most cases lie beyond the values for maximum lift-to-drag ratio. However, thin wings are favourable in order to keep supersonic wave drag due to volume as low as possible. This implies that, in case a range constraint is imposed, an optimum value exists for the thickness-to-chord ratio and the leading-edge radius. In that case, the optimal wing angle of incidence might be taken relatively high if the optimal leading-edges are taken relatively sharp, in order to remain in the favourable region of high lift coefficients. For a given wing area and cruise weight, this might lead to higher cruise altitudes, an effect that in turn will influence engine performance. It might therefore be concluded, that by taking leading-edge suction and vortex flow into account, a very important variable, that is, the leading-edge radius, can be introduced in the process of high-speed civil transport optimization.

For a pure delta wing of unit aspect ratio, the induced drag polars are drawn in fig.13, for the cases of full leading-edge suction, full leading-edge vortex flow and for vortex flow with fifty percent of the theoretical suction force still present. As can be clearly seen, with full leading-edge suction, the drag force is much lower than in case separation occurs. On the other hand, in case full vortex flow occurs, a dramatic increase in lift is possible: in

fig.13 and fig.14 at an angle of attack of 20 degrees, an increase of 50% is achieved. Furthermore, it can be concluded, that the presence of leading-edge vortices can be very advantageous for high wing loading/low aspect ratio vehicles in the low speed regime, especially during take-off and landing. The increase of lift due to leading-edge vortices enables Concorde to land without the use of flaps. This suggests the use of a high lift device with zero leading-edge nose radius, which can be deployed during approach, thus causing a large increase in lift and drag. In fact, the use of similar "vortex slats" is currently studied on the F16 XL aircraft at the NASA Langley Research Centre for possible use on a future High Speed Civil Transport ([ref.1]). On military aircraft, there is an additional application during high wing loading manoeuvres.

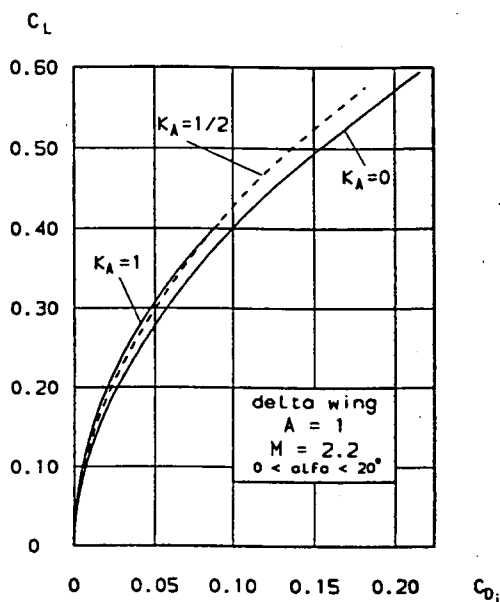


fig.13 drag polars for different values of the attainable thrust coefficient

Since the attainable thrust coefficient depends on the angle of attack, it will normally decrease as the wing is rotated toward higher angles of attack unless full leading-edge suction can be retained under the circumstances. This implies that the leading-edge suction vector rotates backwards with the wing. In order to illustrate this, the induced drag polar and the lift versus angle of attack curve according to the attainable thrust concept, are plotted in fig.14 for the same wing as used previously. The limits for full leading-edge suction and full vortex flow are shown in this figure as well. According to the right-hand figure, the full leading-edge suction force is retained up to an angle of attack of approximately eight degrees. At this point, the curve leaves the line for $K_A = 1$ and bends toward the full vortex flow line which it approaches for high angles of attack.

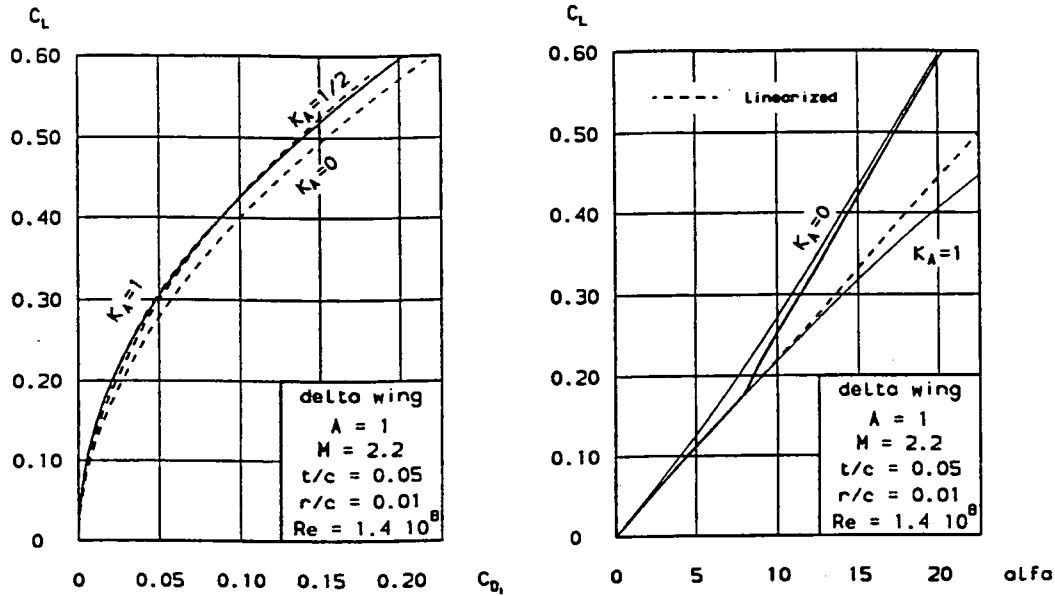


fig.14 drag polar and C_L - α line according to attainable thrust concept

This behaviour is depicted in a somewhat different way in fig.15, in which, again for the same wing, the lift dependent drag factor is plotted against the lift coefficient. Again, the two extreme cases for $K_A=0$ and $K_A=1$ are plotted as well, for both cases the linear as well as the non-linear relation. The linear relation for 100% leading-edge suction is:

$$\frac{C_{D_i}}{C_L^2} = \frac{2E - \sqrt{1 - m^2}}{\pi A} \quad (70)$$

which is independent of the lift coefficient. The linearized relation for the full vortex case depends on the lift coefficient, and so do (trivially) the non-linearized relations. Again, it is clear that for a lift coefficient of approximately 0.20, the curve diverges from the full leading-edge suction line.

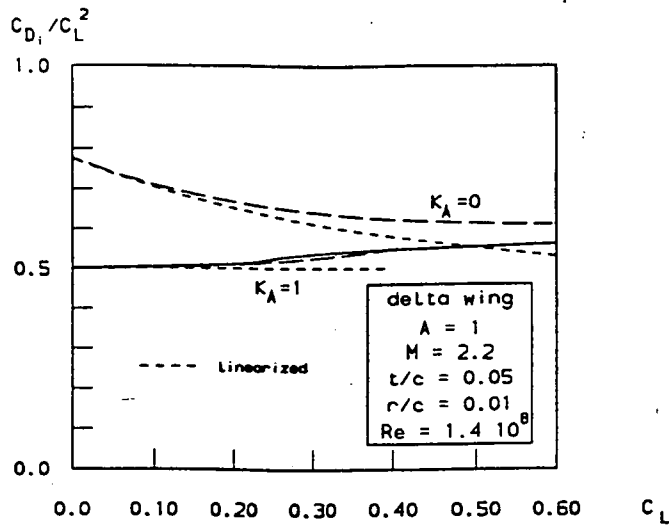


fig.15 induced drag factor as a function of the lift coefficient

A more clarifying picture of the influence of the leading-edge flow on the lift dependent drag is found in fig.16. As far as the linearized equations are concerned, this is an often published figure, in which the lift dependent drag factor divided by πA is plotted against the leading-edge parameter m . The linearized relation for the full leading-edge suction case is simply:

$$\frac{C_{D_i}}{C_L^2/\pi A} = 2E - \sqrt{1 - m^2} \quad (71)$$

The case for no suction (which is only a theoretical one) then becomes:

$$\frac{C_{D_i}}{C_L^2/\pi A} = 2E \quad (72)$$

As soon as the leading-edge becomes sonic, the flow becomes two-dimensional (constant wing loading) and leading-edge suction or vortex flow can no longer occur. At that point the well known linear relations of Ackeret apply:

$$C_L = \frac{4\alpha}{\sqrt{M^2-1}} \text{ and } C_D = \frac{4\alpha^2}{\sqrt{M^2-1}}, \text{ yielding:}$$

$$C_D = \frac{1}{4}\sqrt{M^2-1}C_L^2 \tag{73}$$

This figure clearly illustrates the importance of sufficiently swept wings with sufficiently rounded leading-edges. To reduce the lift dependent drag, high relative wing thicknesses are advantageous too, however, this will negatively affect the wing zero lift wave drag. With the equations derived in this report, curves can be drawn in the figure for the nonlinear full leading-edge suction case and the full vortex case. The increase in drag caused by the vortices is obvious. Since the nonlinear relations are dependent of the angle of attack, they apply for a specified angle of attack only; in this example, for clarity, a relative large value of ten degrees was chosen. Also, in this figure, the line according to the attainable thrust concept was drawn, which closely follows the line for full leading-edge suction.

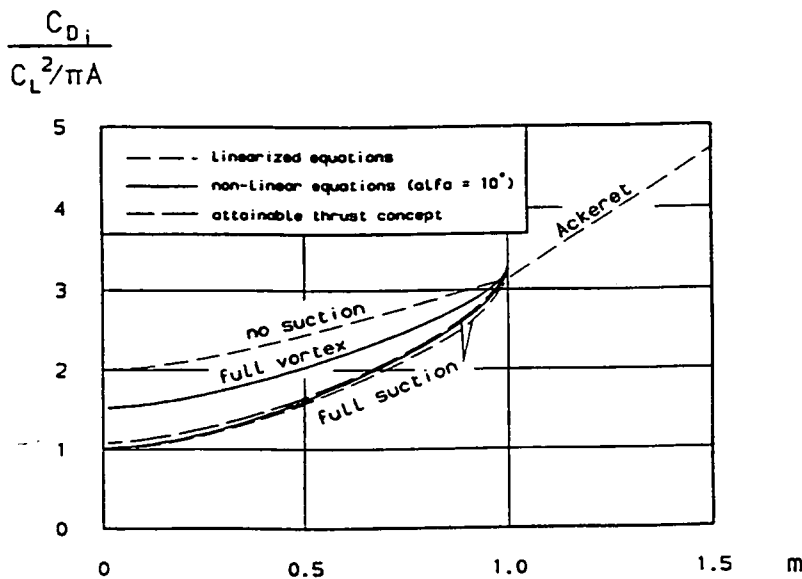


fig.16 induced drag factor for full suction, no suction, full vortex and attainable thrust

The impact of the leading-edge parameter (or aspect ratio for a delta wing at constant Mach number) and the wing nose radius and relative thickness is illustrated in fig.17, where a fuselage (Sears-Haack body of length 60 m. and diameter 5 m.) was added to a wing of constant area (400 m^2) and varying aspect ratio. In this simple example, it is assumed that all volume is carried inside the fuselage (wing zero lift wave drag negligible), whereas all lift is generated by the wing (no fuselage lift induced drag). In the figure the maximum cruise lift-to-drag ratio is plotted against the aspect ratio for the linearized case of full leading-edge suction as well as for the case of full vortex flow. In case of full leading-edge suction, the decrease of the induced drag with increasing aspect ratio and the simultaneous decrease of the leading-edge suction forces leads to an optimal value for the aspect ratio. In case, however, the leading-edge suction force cannot be generated because the wing is too sharp or too thin (in order to reduce volume drag in a practical design), the L/D ratio is drastically reduced due to the occurrence of vortex flow, and no optimum exists for a subsonic leading-edge.

Since the design of a supersonic airplane wing is always a compromise between high-speed and low-speed performance requirements, it is important to be able to analyze the low-speed characteristics of typical supersonic wing designs. With the use of the equations presented in this report, it is possible to analyze the influence of certain parameters on the approach lift coefficient. Delta wings and highly swept wings, if at all, only stall (because of vortex breakdown) at very high angles of attack. Therefore, usually no maximum lift coefficient is defined, but an approach lift coefficient which is based on a maximum allowable approach angle of attack with respect to runway visibility. In this example it is put at 12 degrees. In fig.18 the approach lift coefficient is plotted against the aspect ratio of a family of pure delta wings.

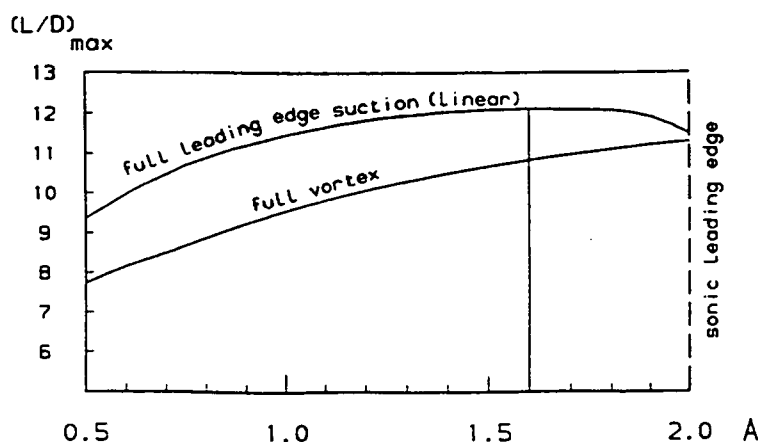


fig.17 effect of aspect ratio on maximum lift-to-drag ratio

The results have been calculated for a Mach number of 0.5 for wings with a relative nose radius of $r/c=0.01$ and a relative thickness of $t/c=0.025$. The subsonic lift gradient was calculated using the following relation from [ref.7]:

$$C_{L\alpha} = \frac{2\pi}{\frac{2}{A} + \left(\frac{(1-M^2)}{\cos^2 \Lambda_{1/2}} + \left(\frac{2}{A} \right)^2 \right)^{1/2}} \quad (74)$$

A constant elliptical span efficiency factor $\phi=0.8$ was used in order to obtain the theoretical subsonic suction force. From the figure it follows, that up to an aspect ratio of 1.5, full leading-edge suction can be retained. If the attainable suction coefficient is artificially set equal to zero (by deploying the vortex slats) the approach lift coefficient increases, as expected. It should be realized, however, that this is by no means trivial. If for a certain wing at angle of attack, the attainable thrust coefficient happens to be such that the upward rotated suction force vector points exactly vertical, then setting the attainable suction coefficient equal to zero will cause the vector to rotate backwards until it acts perpendicular to the wing chord, leading to a decrease in the vertical resultant. Using the relations from this report, this effect can be investigated by examining the ratio of the increase in lift coefficient with respect to the two-dimensional potential flow contribution, with and without vortex slats deployed:

$$\frac{\Delta C_{L_{K_A > 0}}}{\Delta C_{L_{K_A = 0}}} = \frac{K_A K_T}{K_V} \tan \alpha + \sqrt{1 - K_A^2} \quad (75)$$

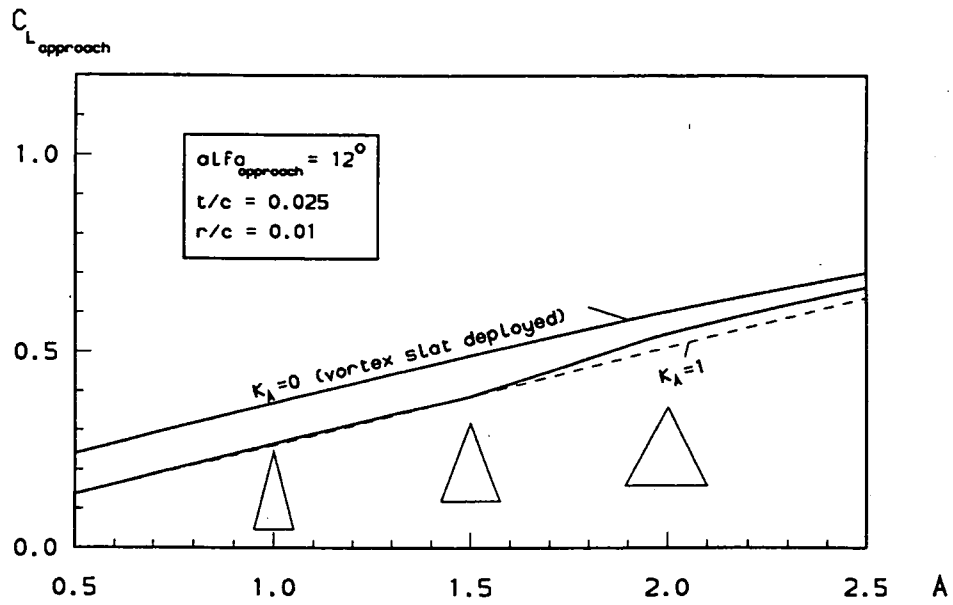


fig.18 effect of deploying vortex slat on approach lift coefficient

6. Conclusions

The methods presented in this report enable the designer to account for the influence of leading-edge vortices on the lift and drag coefficient of flat delta wings and derived planforms, both at subsonic and supersonic speeds. Without this method, this effect which is extremely important for any supersonic airplane design or optimization study, could not as easy (and as cheap) be taken into account at the earliest stage of conceptual design.

No validation or verification of the method has been carried out in this report, since the presented method is a combination of two established methods integrated over the wing span, methods which have demonstrated the capability to capture the non-linear effects very well.

References

1. Aviation Week & Space Technology
September 13, 1993, pp. 50-52
2. Brown, C.E.
Theoretical Lift and Drag of Thin Triangular Wings at Supersonic Speeds
NACA Rept. No. 839, November, 1946
3. Carlson, H.W. and Mack, R.J.
Estimation of Leading-Edge Thrust for Supersonic Wings of Arbitrary Planform
NASA TP 1270, October 1978
4. Carlson, H.W.; Mack, R.J. and Barger, R.L.
Estimation of Attainable Leading-Edge Thrust for Wings at Subsonic and Supersonic Speeds
NASA TP 1500, October 1979
5. Carlson, H.W. and Mack, R.J.
Studies of Leading-Edge Thrust Phenomena
Journal of Aircraft Vol. 17, No. 12, December 1980
6. Carlson, H.W. and Miller, D.S.
Influence of Leading-Edge Thrust on Twisted and Cambered Wing Design for Supersonic Cruise
Journal of Aircraft Vol. 20, No. 5, May 1983
7. Hoak, D.E.
USAF Stability and Control DATCOM
2nd ed., 1968
8. Hoeijmakers, H.W.M.
A panel method for the determination of the aerodynamic characteristics of complex configurations in linearized subsonic and supersonic flow
National Aerospace Laboratory NLR,
NLR TR 80124 U, part 1,2,3, December 1980
9. Hoeijmakers, H.W.M.
National Aerospace Laboratory NLR,
Memorandum AT-83-005 U, November 1983
10. Hutchison, M.G.; Huang, X.; Mason, W.H.; Haftka, R.T. and Grossman, B.
Variable-Complexity Aerodynamic-Structural Design of a High-Speed Civil Transport Wing
AIAA 92-4695, September 1992

11. Middel, J.
Development of a Computer Assisted Toolbox for Aerodynamic Design of Aircraft at Subcritical Conditions with Application to Three-Surface Aircraft
PhD. Thesis, ISBN 90-6275-768-5/CIP
Delft University Press, 1992
12. Polhamus, E.C.
A Concept of the Vortex Lift of Sharp-Edge Delta Wings Based on a Leading-Edge Suction Analogy
NASA TN D-3767, October 1966
13. Polhamus, E.C.
Prediction of Vortex Lift Characteristics by a Leading-Edge Suction Analogy
Journal of Aircraft Vol.8, No.4, April 1971
14. Schlichting, H. and Truckenbrodt, E.
Aerodynamik des Flugzeuges
Springer Verlag, Berlin 1960

Appendix

Calculation of spanwise coordinates for mean attainable thrust coefficient

pure delta wings

According to equation (51), in order to use the mean attainable thrust coefficient as a factor on the suction force coefficient for full suction (equation (54)), it must be equal to:

$$K_A = \frac{8}{b^2} C \int_0^{b/2} y^{2/5} dy = \frac{C}{\bar{y}^{3/5}} \quad (A1)$$

in which K_A was written in accordance with equation (39) as a constant C times $y^{-3/5}$.

This yields after solving the integral: $\bar{y} = \left(\frac{7}{40} 2^{7/5} \right)^{5/3} b = 0.276 b = 0.552 s_w$

double delta wings

For double delta wings, the integration of the local suction force coefficient is carried out in two parts, over the inner and over the outer wing panel. Using again equation (28) for the local suction force coefficient and writing $K_A = C \cdot y^{-3/5}$ the following expression for the attainable thrust coefficient on the inner wing panel is obtained:

$$C_{T_{A_i}} = \frac{\pi A}{4E_i^2} \sqrt{1 - m_i^2} \sin^2 \alpha \frac{8C}{b^2} \int_0^{l_i} y^{2/5} dy = K_{T_i} K_A \sin^2 \alpha \quad (A2)$$

After substituting equation (63), this yields for the mean value of the attainable thrust coefficient of the inner wing panel:

$$K_{A_i} = \frac{2}{l_i^2} C \int_0^{l_i} y^{2/5} dy = \frac{C}{\bar{y}_i^{3/5}} \quad (A3)$$

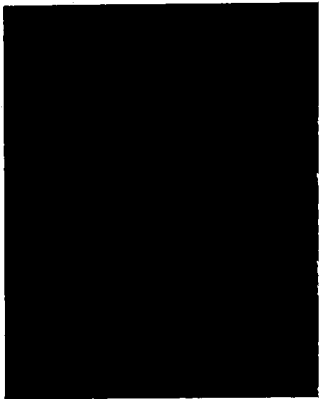
After solving the integral, this yields: $\bar{y}_i = 0.552 l_i$.

For the outer panel follows in the same way, using equation (64):

$$\bar{K}_{A_o} = \frac{2}{s_w^2 \left(1 - \left(\frac{l_i}{s_w} \right)^2 \right)} C \int_0^{s_w} y^{2/5} dy = \frac{C}{\bar{y}_o^{3/5}} \quad (\text{A4})$$

After solving the integral, this yields for the spanwise coordinate on which the mean attainable thrust coefficient of the outer panel must be based:

$$\bar{y}_o = 0.552 s_w \left(\frac{1 - \left(\frac{l_i}{s_w} \right)^2}{1 - \left(\frac{l_i}{s_w} \right)^{7/5}} \right)^{5/3} \quad (\text{A5})$$



(17)

Rapport 779



60141010795

947874